Time-resolved laser-induced fluorescence lifetime measurements and theoretical transition probabilities in Tb III

E. Biémont,[1,2] H. P. Garnir,[2] P. Quinet,[1,2] S. Svanberg,[3] and Z. G. Zhang[3]
[1]*Astrophysique et Spectroscopie, Université de Mons-Hainaut, B-7000 Mons, Belgium*
[2]*IPNAS (Bâtiment B15), Université de Liège, Sart Tilman, B-4000 Liège 1, Belgium*
[3]*Department of Physics, Lund Institute of Technology, P.O. Box 118, S-221 00 Lund, Sweden*
(Received 2 January 2002; published 18 April 2002)

Lifetimes of four short-lived levels belonging to the $4f^8(^7F)6p$ configuration of Tb III have been measured using a two-step excitation time-resolved laser-induced fluorescence technique. They agree quite well with multiconfigurational relativistic Hartree-Fock calculations performed with inclusion of core-polarization effects. Using the experimental lifetimes and the theoretical branching fractions, a set of transition probabilities has been deduced for this ion.

DOI: 10.1103/PhysRevA.65.052502 PACS number(s): 32.70.Cs, 42.62.Fi

I. INTRODUCTION

The increasing interest in the spectra of doubly and trebly ionized rare-earth (RE) elements results partly from their connection with the crystal spectra of the divalent and trivalent RE salts. In fact, the comparison of the levels of the crystals with those of the free ions helps in a better understanding of the crystal forces that are responsible for a modification of the levels of the ion inside the crystals. These show complicated absorption and fluorescence spectra due to the multiplicity of the levels originating from the $4f^n$ configurations. It is clear, from these considerations, that the lanthanide ions can be used as a sensitive probe of crystalline structure of RE salts [1].

In astrophysics, the study of the composition of chemically peculiar (CP) stars reveals large overabundances of RE elements when they are compared with the chemical composition of the Sun (see, e.g., [2]). Rather limited information, however, is available concerning the occurrence of third spectra of lanthanides in stellar sources, although their presence in some stars has long been recognized (see, e.g., [3]). Doubly ionized terbium (Tb III) has been particularly little considered up to now in this context. The reason is that, although the strongest line of this ion appears to be present in the spectrum of some stars (e.g., HR 465 and HD 25354), not enough additional lines are identified to appraise the significance of the identification [4]. Adelman and Shore [5], however, showed that Tb III was possibly present in the International Ultraviolet Explorer spectra of HD 51418, but this ion was not identified [6] in other CP stars. Tb III has been identified in Przybylski's star, which shows strong lines for the lanthanide ions when compared to the iron group elements, frequently dominant in ''normal'' stars. Although the identifications may be obscured by some blending problems, there is no reason to believe that the abundance of this element departs from the odd-even effect which is generally observed for the REs. A possible explanation is the hyperfine structure, but the more likely one is the fact that this element might be a factor of 5 or so less abundant than its even-*Z* neighbors. This point needs to be clarified on the basis of accurate atomic oscillator strengths.

Transition probabilities, if available, could also help for a more quantitative analysis of Tb III spectrum in the laboratory. Until now, however, no transition probabilities (either theoretical or experimental) are available for this ion, although such data are needed in plasma physics. Consequently, in this work, we report lifetime measurements of four levels of Tb III using time-resolved laser-induced fluorescence spectroscopy and a laser-produced plasma. Experimental data are compared with theoretical calculations performed within the framework of a relativistic Hartree-Fock (HFR) approach [7] including configuration-interaction and core-polarization (CP) effects. This comparison allows one to test the accuracy of the oscillator strengths of the transitions originating from four levels belonging to the $4f^86p$ configuration and to derive a set of transition probabilities for this ion from a combination of the experimental lifetimes and the theoretical branching ratios.

The present work is part of an extensive program of lifetime measurements in doubly ionized REs. The results obtained so far concern the following ions: La III–Lu III [8], Ce III [9], Gd III [10], Er III [11], Pr III [12,13], Tm III [14], Yb III [15,16], Eu III [17], Nd III [18], and Ho III [19,20]. See also the database of astrophysical interest, database on rare earths at Mons University (DREAM) [30] where extensive sets of transition probabilities are stored.

II. EXPERIMENTAL LIFETIME MEASUREMENTS

In the present work, the lifetimes of four levels belonging to the configuration $4f^86p$ were measured with a two-step excitation time-resolved laser-induced fluorescence technique applied to a laser-produced plasma. The experimental schemes are summarized in Table I.

The experimental arrangements used in the experiments have been described elsewhere (see, e.g., [10–12,15,16,18–20]). Free Tb^{2+} ions were obtained by laser ablation. Laser pulses, characterized by a 532 nm wavelength, a 10 Hz repetition rate, and a 10 ns duration, were emitted from a neodymium-doped yttrium aluminum garnet (Nd:YAG) laser (Continuum Surelite). The pulses, usually of energy in the 2–5 mJ range, were focused vertically onto the surface of a pure terbium foil, which was rotated in a vacuum chamber. After the pulses, a plasma containing Tb atoms and ions in different ionization stages expanded from the foil with different speeds. When Tb^{2+} ions, moving faster than Tb^+ ions

TABLE I. Excitation schemes in Tb III.

Measured level[a] (cm^{-1})		Origin level[a] (cm^{-1})	λ_{exc} (nm)	λ_{obs} (nm)	Nonlinear scheme[b]
$4f^8(^7F_5)6p_{1/2}(5,1/2)^o_{11/2}$	54 632.46	16 261.84	260.54	291.3	$2\nu+2S$
$4f^8(^7F_5)6p_{3/2}(5,3/2)^o_{11/2}$	58 811.23	16 261.84	234.95	261.7	$3\nu+S$
$4f^8(^7F_5)6p_{3/2}(5,3/2)^o_{13/2}$	59 189.83	16 261.84	232.88	257.2	$3\nu+S$
$4f^8(^7F_4)6p_{3/2}(4,3/2)^o_{11/2}$	60 687.12	16 261.84	225.03	261.6	$3\nu+S$

[a]Energy levels from [24].

[b]ν means the frequency of a DCM dye laser: S or $2S$ means the first or the second Stokes component; 3ν means frequency tripling.

and Tb atoms, reached the interaction zone at 1 cm above the foil, they were excited with suitable lasers into the levels under study.

Two lasers were used to populate the ionic levels of interest in the experiment. First, a dye laser set with a wavelength of 614.767 nm, pumped by a Continuum NY-82 Nd:YAG laser with a pulse energy of 600 mJ and a repetition rate of 10 Hz, was employed to populate the intermediate level 16 261.84 cm^{-1} belonging to the configuration $4f^85d$. This laser, used as the first-step excitation light source, was sent horizontally to the center of the vacuum chamber, where it interacted with the ions. In order to excite the ions in the intermediate state to the levels measured, an injection-seeded Nd:YAG laser (Continuum NY-82) with a pulse duration of 8 ns, a repetition rate of 10 Hz, and a single laser pulse (energy of 400 mJ) was shortened with a stimulated Brillouin scattering cell down to 1 ns. The pulse was used to pump a dye laser (Continuum Nd-60), in which a DCM dye was used. The dye laser pulse was subsequently frequency tripled in a nonlinear optical system, consisting of a potassium dihydrogen phosphate crystal, a retarding plate, and a β-barium borate (BBO) crystal. According to the excitation requirements, shown in Table I, different-order Stokes stimulated Raman scattering components of the third-harmonic radiation were produced by focusing the harmonic radiation into a hydrogen conversion cell with a gas pressure of about 10 bars. The light of interest was selected using a quartz Pellin-Broca prism. The laser beam was also sent horizontally into the vacuum chamber in order to cross the first-step excitation laser beam above the foil.

The three Nd:YAG lasers used in the experiments were triggered externally by two digital delay generators (Stanford Research System model 535), which were connected mutually and employed to adjust the delay time between the two excitation pulses and the timing with regard to the ablation pulse. By properly choosing trigger parameters for the lasers, Tb^{2+} ions were excited to the levels of interest when the ions reached the interaction zone. In the lifetime measurements, the first-step excitation pulse arrived at the ions about 20 ns earlier than the second-step excitation pulse. Fluorescence from the measured levels was imaged by two MgF_2 lenses onto the entrance slit of a vacuum monochromator, and the fluorescence selected by the monochromator was detected by a Hamamatsu R3809-58 photomultiplier. The time-resolved signal was acquired and averaged employing a digital transient recorder (Tektronix model DSA 602), and the averaged time-resolved fluorescence decay curve was sent to a personal computer for subsequent lifetime evaluation.

A detailed discussion of this type of measurements can be found elsewhere (see, e.g., [10–12,15,16,18–20]); only a brief account is given here. Before the measurements, a careful check was made to verify that there were no identified lines belonging to neutral Tb atoms and Tb^+ ions in the spectral neighborhood of the excitation wavelengths given in Table I, and the ionic stage identification was further supported by studying the temporal behavior of the signals related to the plasma conditions. A magnetic field of about 120 G was added over the plasma zone by a pair of Helmholtz coils to reduce the plasma background light accompanying the signal recording. The background, nearly invisible after applying the field, is due to recombination between the ions and electrons in the plasma. The effect of the field is to cause the ions and the electrons to move in orbits of widely different radii, keeping them spatially separated.

In the measurements, the entrance slit of the monochromator was placed horizontally and opened maximally in order to efficiently collect the fluorescence. In order to obtain a smooth decay curve with a reasonable signal-to-noise ratio in the measurements, the curve was recorded by averaging fluorescence photons from more than 4000 pulses. During the experiments, a variety of experimental conditions were

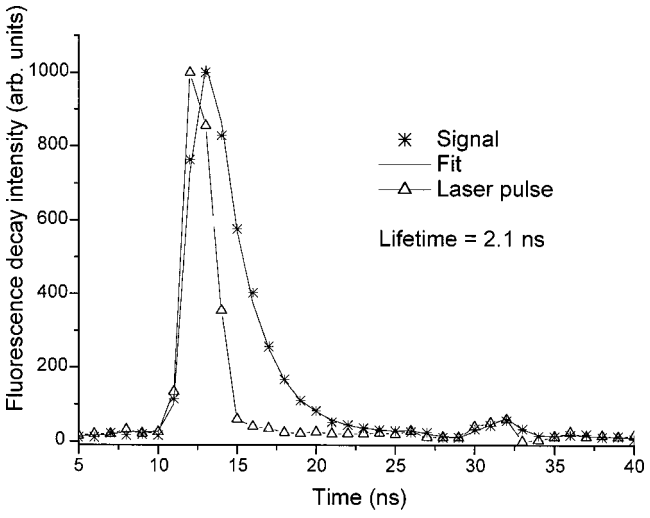

FIG. 1. A typical experimental time-resolved fluorescence signal from the level at 54 632.46 cm^{-1} in Tb III. The lifetime deduced from the fit was 2.1 ns.

changed, including the intensity of the excitation laser, that of the ablation laser, and the delay time, which resulted in a modification of temperature and ionic density in the plasma. This resulted in a change of the fluorescence signal intensity by a factor of 4, but it was found that the lifetime values had no clear covariation. The lifetime evaluation was performed by fitting the fluorescence signal with a convolution of the detected excitation laser pulse and an exponential function with adjustable parameters. A typical curve is shown in Fig. 1. About 10 curves were recorded for each level investigated, and the final lifetime result for each level was taken as the average of the data for the curves. The electronic bandwidth limitations of the detection system used in the present work were recently tested [9] by considering the lifetime of the short-lived Be I $2s2p\ ^1P_1^o$ level. The lifetime obtained, i.e., 1.79(10) ns, for this level was found in excellent agreement with previous theoretical [21] and experimental [22] results.

The four deduced lifetimes are shown in the last column of Table II, where the error bars reflect not only the statistical errors but also a conservative estimate for possible remaining systematic errors. We give also in the same table the theoretical lifetime values obtained according to the procedure described in Sec. III hereafter.

III. CALCULATIONS OF LIFETIMES AND OF OSCILLATOR STRENGTHS

Terbium ($Z=65$) has only one stable isotope (^{159}Tb) and 23 short-lived isotopes and isomers. Doubly ionized terbium (Tb III) belongs to the europium isoelectronic sequence, a complex atomic structure of the lanthanide series. Its fundamental configuration is $4f^9$ and the only experimentally known excited configurations are $4f^8nl$ ($nl=5d$, $6s$, and $6p$).

The laboratory spectrum of doubly ionized terbium has been produced by a pulsed hollow-cathode source and the spectrum analyzed [23]. At that time, 485 transitions were classified among the 2500 lines observed. They connect the $4f^8(^7F)5d$ configuration to the lowest ^6H and ^6F terms of the ground configuration $4f^9$ and also the $4f^8(^7F)6p$ con-

TABLE II. Experimental and theoretical radiative lifetimes (in ns), for the $4f^86p$ levels of Tb III. The theoretical values have been obtained without (HFR) and with (HFR+CP) inclusion of core-polarization effects.

Level	J	E (cm^{-1})	HFR[a]	HFR+CP[a]	Experiment[a]
$4f^8(^7F_6)6p_{1/2}(6,1/2)^o$	11/2	52 039.185	1.48	1.96	
	13/2	52 252.635	1.48	1.95	
$4f^8(^7F_5)6p_{1/2}(5,1/2)^o$	9/2	53 831.125	1.45	1.92	
	11/2	54 632.46	1.56	2.06	2.1±0.1
$4f^8(^7F_4)6p_{1/2}(4,1/2)^o$	7/2	54 965.075	1.44	1.90	
	9/2	55 932.24	1.62	2.14	
$4f^8(^7F_3)6p_{1/2}(3,1/2)^o$	5/2	55 705.84	1.44	1.90	
	7/2	56 857.39	1.56	2.06	
$4f^8(^7F_6)6p_{1/2}(6,3/2)^o$	13/2	56 779.125	1.21	1.60	
	15/2	57 036.08	1.07	1.41	
	11/2	57 620.57	1.23	1.62	
	9/2	58 722.65	1.30	1.72	
$4f^8(^7F_2)6p_{1/2}(2,1/2)^o$	5/2	57 433.545	1.56	2.06	
$4f^8(^7F_1)6p_{1/2}(1,1/2)^o$	3/2	57 773.445	1.51	2.00	
$4f^8(^7F_0)6p_{1/2}(0,1/2)^o$	1/2	57 893.975	1.49	1.97	
$4f^8(^7F_5)6p_{3/2}(5,3/2)^o$	11/2	58 811.23	1.15	1.52	1.6±0.1
	13/2	59 189.825	1.11	1.47	1.4±0.1
	9/2	59 712.255	1.21	1.60	
	7/2	60 440.755	1.30	1.72	
$4f^8(^7F_4)6p_{3/2}(4,3/2)^o$	9/2	60 089.475	1.12	1.48	
	11/2	60 687.115	1.16	1.54	1.4±0.2
	7/2	61 009.61	1.21	1.61	
	5/2	61 435.10	1.30	1.72	
$4f^8(^7F_3)6p_{3/2}(3,3/2)^o$	7/2	61 131.515	1.11	1.46	
	9/2	61 847.625	1.20	1.58	
	5/2	61 973.18	1.20	1.58	
$4f^8(^7F_2)6p_{3/2}(2,3/2)^o$	5/2	62 157.57	1.12	1.48	
	7/2	62 733.445	1.23	1.62	
$4f^8(^7F_1)6p_{3/2}(1,3/2)^o$	5/2	63 383.965	1.25	1.65	
	3/2	63 721.245	1.27	1.68	

[a]This work (see text).

TABLE III. Numerical values (in cm^{-1}) adopted in this work for the radial parameters of the $4f^9$, $4f^8 6p$ odd-parity and the $4f^8 5d$, $4f^8 6s$ even-parity configurations of Tb III. The ratios between fitted and *ab initio* values are also given in the table.

Configuration	Parameter	Adopted value (cm^{-1})	Ratio
$4f^9$	E_{av}	46854	
	$F^2(4f,4f)$	77482	0.691
	$F^4(4f,4f)$	59461	0.580[a]
	$F^6(4f,4f)$	42691	0.850[a]
	ζ_{4f}	1557	0.943
$4f^8 6p$	E_{av}	126309	
	$F^2(4f,4f)$	102069	0.850[a]
	$F^4(4f,4f)$	64044	0.850[a]
	$F^6(4f,4f)$	46076	0.850[a]
	ζ_{4f}	1698	0.954
	ζ_{6p}	3213	1.237
	$F^2(4f,6p)$	6232	0.846
	$G^2(4f,6p)$	1830	0.982
	$G^4(4f,6p)$	1491	0.893
$4f^8 5d$	E_{av}	85352	
	$F^2(4f,4f)$	101537	0.850[a]
	$F^4(4f,4f)$	63685	0.850[a]
	$F^6(4f,4f)$	45811	0.850[a]
	ζ_{4f}	1702	0.960
	ζ_{5d}	1063	0.980
	$F^2(4f,5d)$	20919	0.822
	$F^4(4f,5d)$	10366	0.859
	$G^1(4f,5d)$	7396	0.646
	$G^3(4f,5d)$	5786	0.630
	$G^5(4f,5d)$	5879	0.843
$4f^8 6s$	E_{av}	89166	
	$F^2(4f,4f)$	102008	0.850[a]
	$F^4(4f,4f)$	64003	0.850[a]
	$F^6(4f,4f)$	46046	0.850[a]
	ζ_{4f}	1689	0.950
	$G_3(4f,6s)$	2213	0.810

[a]Parameter fixed to 85% of its *ab initio* value (see text).

figuration to $4f^8(^7F)6s + 4f^8(^7F)5d$ in the spectral range 200.0–680.0 nm.

The NIST compilation [24] lists 101 energy levels belonging essentially to the configurations $4f^9$, $4f^8(^7F)5d$, $4f^8(^7F)6s$, and $4f^8(^7F)6p$. Two additional levels [at 56 970.345 ($J=11/2$) and 59 837.625 ($J=9/2$) cm^{-1}] have been determined by Wyart [25] who also published a list containing the 59 strongest transitions of Tb III located in two different spectral regions, some of them showing hyperfine structure effects.

Atomic structure calculations in a heavy and low-ionized atom, such as Tb III, are extremely complex. The simultaneous consideration, in the theoretical models, of both intravalence and core-valence interactions is crucial when performing calculations. These considerations apply also to most of the RE ions, as frequently pointed out in recently (see, e.g., [8,9,11–15]).

In view of the huge matrix dimensions involved in the calculations, which are basically limited by the available computer capabilities, we were only able to consider explicitly, in the HFR model, the experimentally known configurations, i.e., $4f^9 + 4f^8 6p$ for the odd parity, and $4f^8 5d + 4f^8 6s$ for the even parity. This set of configurations represents a total of 5194 possible energy levels. Due to the limited computer capabilities, we were not able to include the $4f^7 5d^2$ configuration in the calculation although this configuration is expected to overlap the known levels of $4f^8 6p$. Indeed, according to Brewer [26], the lowest energy level of $4f^7 5d^2$, i.e., $4f^7(^8S^o)5d^2\ ^{10}F^o_{3/2}$, should appear at $51\,000 \pm 9000\ cm^{-1}$ while the lowest $4f^8 6p$ level $[4f^8(^7F_6)6p_{1/2}(6,1/2)^o_{11/2}]$ has been identified at 52 039.185 cm^{-1} [24]. The limited set of configurations adopted in the theoretical model is, however, realistic because it is well established (see, e.g., [27]) that the $4f^n 6s$ and $4f^n 6p$ levels of the third spectra of the rare earths do not interact strongly with other configurations, and that the radial energy integrals for these configurations are nearly constant along the period.

The core-valence correlation was introduced via a model potential and a correction to the dipole operator (see, e.g., [13]). In order to consider these effects in the $4f^8 nl$ type configurations, we used a dipole polarizability α_d equal to $6.55 a_0^3$ which corresponds to the tabulated value [28] for Tb IV. The cutoff radius r_c was taken as the HFR mean radius of the outermost core orbital, i.e., $\langle 5p|r|5p\rangle = 1.52 a_0$ which corresponds to the HFR average value $\langle r\rangle$ for the outermost core orbitals ($5p^6$) of the investigated configurations. The transitions considered here are essentially of the type $5d$-$6p$ and $6s$-$6p$ and, for such transitions, the approach followed for expressing the CP effects should be entirely adequate.

CP effects were taken into account neither in the fundamental configuration calculation nor in the $\langle 4f|r|5d\rangle$ transition matrix element calculation. In most lanthanide ions, the $4f$ orbital is actually deeply imbedded inside the Xe-like core and so the analytical treatment used for the excited configurations is generally no longer valid with the consequence that the $4f$-$5d$ transitions deserve a special treatment. A possibility to solve this problem, originating from the fact that the analytical core-polarization and core-penetration corrections to the dipole operator are no longer valid, consists in applying an empirical scaling factor to the uncorrected $\langle 4f|r|5d\rangle$ radial matrix element [29]. However, the introduction of this scaling factor was not attempted in the present work because no radiative lifetimes were accessible to the experiment for the even-parity levels (all of them being greater than 350 ns according to our calculation) and, consequently, it was not possible to test the introduction of the semiempirical correction factor needed for the radial matrix element.

The HFR method was combined with a least-squares optimization process minimizing the differences between the experimental energy levels [24] and the eigenvalues of the Hamiltonian matrix. Six levels above 50 000 cm^{-1}, i.e.,

TABLE IV. Oscillator strengths ($\log_{10} gf$) and transition probabilities [gA (s^{-1})] of the most intense lines ($\log_{10} gf > -1.0$) of Tb III depopulating the levels for which the lifetimes have been measured in the present work. Numbers in brackets represent powers of 10.

λ (nm)	Lower level[a]			Upper level[a]			$\log_{10} gf$[b]	gA[b]
199.1336	8 972	(*e*)	13/2	59 190	(*o*)	13/2	−0.87	2.28[8]
200.5814	8 972	(*e*)	13/2	58 811	(*o*)	11/2	−0.99	1.69[8]
216.3667	12 987	(*e*)	13/2	59 190	(*o*)	13/2	−0.37	6.14[8]
217.7208	14 771	(*e*)	11/2	60 687	(*o*)	11/2	−0.77	2.40[8]
218.1545	12 987	(*e*)	13/2	58 811	(*o*)	11/2	−0.20	8.87[8]
224.3364	10 070	(*e*)	9/2	54 632	(*o*)	11/2	−0.83	1.94[8]
225.0273	16 262	(*e*)	13/2	60 687	(*o*)	11/2	−0.41	5.22[8]
226.9956	14 771	(*e*)	11/2	58 811	(*o*)	11/2	−0.32	6.18[8]
227.5681	16 758	(*e*)	11/2	60 687	(*o*)	11/2	−0.89	1.66[8]
228.9034	15 517	(*e*)	15/2	59 190	(*o*)	13/2	−0.07	1.08[9]
230.2660	11 218	(*e*)	11/2	54 632	(*o*)	11/2	−0.24	7.13[8]
232.8768	16 262	(*e*)	13/2	59 190	(*o*)	13/2	−0.90	1.56[8]
234.9490	16 262	(*e*)	13/2	58 811	(*o*)	11/2	−0.14	8.73[8]
240.0463	12 987	(*e*)	13/2	54 632	(*o*)	11/2	−0.44	4.23[8]
240.8119	17 676	(*e*)	13/2	59 190	(*o*)	13/2	−0.80	1.82[8]
240.8557	19 181	(*e*)	11/2	60 687	(*o*)	11/2	−0.94	1.35[8]
243.6448	18 159	(*e*)	13/2	59 190	(*o*)	13/2	−0.56	3.11[8]
245.1135	19 902	(*e*)	11/2	60 687	(*o*)	11/2	−0.48	3.67[8]
245.9140	18 159	(*e*)	13/2	58 811	(*o*)	11/2	−0.87	1.47[8]
247.4893	18 796	(*e*)	15/2	59 190	(*o*)	13/2	0.18	1.64[9]
247.6369	20 318	(*e*)	11/2	60 687	(*o*)	11/2	−0.47	3.63[8]
249.6867	20 649	(*e*)	9/2	60 687	(*o*)	11/2	0.00	1.07[9]
249.7080	18 777	(*e*)	9/2	58 811	(*o*)	11/2	−0.99	1.09[8]
249.8701	19 181	(*e*)	11/2	59 190	(*o*)	13/2	0.06	1.24[9]
251.5175	20 940	(*e*)	13/2	60 687	(*o*)	11/2	0.21	1.70[9]
252.2574	19 181	(*e*)	11/2	58 811	(*o*)	11/2	−0.55	2.94[8]
256.9317	19 902	(*e*)	11/2	58 811	(*o*)	11/2	−0.58	2.67[8]
257.1760	20 318	(*e*)	11/2	59 190	(*o*)	13/2	0.60	4.02[9]
259.7056	20 318	(*e*)	11/2	58 811	(*o*)	11/2	0.00	9.79[8]
259.8635	22 217	(*e*)	11/2	60 687	(*o*)	11/2	−0.92	1.19[8]
260.5382	16 262	(*e*)	13/2	54 632	(*o*)	11/2	−0.14	7.12[8]
261.6213	22 475	(*e*)	9/2	60 687	(*o*)	11/2	0.52	3.26[9]
261.9609	20 649	(*e*)	9/2	58 811	(*o*)	11/2	0.40	2.41[9]
263.9769	20 940	(*e*)	13/2	58 811	(*o*)	11/2	−0.79	1.53[8]
268.7739	17 438	(*e*)	11/2	54 632	(*o*)	11/2	−0.90	1.16[8]
274.0902	18 159	(*e*)	13/2	54 632	(*o*)	11/2	−0.90	1.13[8]
275.1286	22 475	(*e*)	9/2	58 811	(*o*)	11/2	−0.73	1.64[8]
281.9936	19 181	(*e*)	11/2	54 632	(*o*)	11/2	−0.20	5.26[8]
291.3336	20 318	(*e*)	11/2	54 632	(*o*)	11/2	0.19	1.21[9]
294.1747	20 649	(*e*)	9/2	54 632	(*o*)	11/2	−0.20	4.88[8]
296.7193	20 940	(*e*)	13/2	54 632	(*o*)	11/2	−0.78	1.27[8]
310.8829	22 475	(*e*)	9/2	54 632	(*o*)	11/2	−0.05	6.30[8]

[a]Upper and lower levels of the transitions taken from Ref. [24]. We give the energy level (in cm^{-1}), the parity (*e*) even or (*o*) odd, and the J value.

[b]HFR+CP results (this work) normalized by the laser measurements of the present work (see text).

56 025.375 ($J=3/2$), 56 474.84 ($J=7/2$), 56 694.12 ($J=5/2$), 57 134.15 ($J=3/2$), 61 883.195 ($J=5/2$), and 62 578.475 ($J=5/2$) cm^{-1}, for which no spectroscopic designations are given in the NIST compilation [24], were not considered for the fitting procedure. As already mentioned by Wyart [25], the first three levels could eventually belong to the $4f^7 5d^2$ configuration, which was not included in our physical model. All the radial parameters of the $4f^9$, $4f^8 6p$, $4f^8 5d$, and $4f^8 6s$ were adjusted semiempirically except the $F^4(4f,4f)$ and $F^6(4f,4f)$ integrals in $4f^9$ and the

TABLE V. Theoretical (this work) E_{theor} and experimental E_{expt} energy levels [24] (in cm^{-1}) and calculated Landé g factors (this work) for the low-lying levels ($E<20\,000\ \text{cm}^{-1}$) of Tb III.

J	E_{expt}	E_{theor}	g_{calc}	J	E_{expt}	E_{theor}	g_{calc}
	Odd parity levels				Even parity levels		
5/2	8 285.885	8 285	0.304	9/2	10 070.38	10 085	1.498
5/2	10 220.38	10 274	1.308	9/2	11 752.295	12 055	1.566
7/2	7 422.21	7 415	0.834	9/2	15 278.90	15 150	1.599
7/2	9 144.98	9 148	1.386	9/2	17 169.285	16 961	1.223
9/2	6 258.08	6 245	1.073	9/2	18 761.675	18 612	1.720
9/2	7 621.565	7 620	1.422	9/2	18 776.53	18 787	1.436
11/2	4 734.52	4 725	1.206	11/2	9 218.63	9 226	1.496
11/2	6 470.11	6 419	1.444	11/2	11 217.785	11 572	1.537
13/2	2 804.67	2 800	1.277	11/2	14 771.12	14 774	1.555
15/2	0.00	34	1.326	11/2	16 757.805	16 567	1.310
				11/2	17 437.515	17 450	1.441
				11/2	19 181.10	19 233	1.516
	Even parity levels			11/2	19 902.04	19 824	1.344
1/2	12 454.365	12 558	−1.173	13/2	89 72.29	8 934	1.467
3/2	12 165.155	12 237	1.027	13/2	12 986.505	12 713	1.505
3/2	14 515.35	14 455	2.045	13/2	16 261.835	16 098	1.351
5/2	11 678.865	11 711	1.343	13/2	17 676.265	17 708	1.530
5/2	13 689.615	13 825	1.746	13/2	18 158.91	18 064	1.377
5/2	16 066.485	16 242	1.905	15/2	9 275.42	9 369	1.458
5/2	17 755.55	17 533	0.707	15/2	15 516.735	15 393	1.377
7/2	10 996.01	11 002	1.446	15/2	18 796.25	18 789	1.340
7/2	12 775.40	13 036	1.630	17/2	14 890.375	14 888	1.407
7/2	15 820.87	15 840	1.687				
7/2	17 499.43	17 284	1.062				

$F^k(4f,4f)$ $(k=2,4,6)$ parameters in $4f^8nl$ $(nl=6p,5d,6s)$ in relation with the fact that only two terms ($^6F^o$ and $^6H^o$) are known in $4f^9$ and only the ^7F parent term is known in the $4f^8nl$ configurations. Instead, these parameters were fixed to 85% of their *ab initio* values. The mean deviations of the fits were found to be equal to 62 cm^{-1} for the odd parity (40 levels fitted with nine adjustable parameters) and 97 cm^{-1} for the even parity (65 levels fitted with 11 variable parameters). The α, β, and γ parameters, which represent some $4f^9$ core corrections and which are expected to carry out part of the interactions with distant configurations not introduced explicitly in the model, have been kept fixed to zero, in view of the small number of known core terms and of the sensitivity of these parameters to the choice of the configurations introduced explicitly in the model. The numerical values adopted in the present work for the radial integrals are given in Table III.

Experimental and theoretical radiative lifetimes obtained in the present study are compared in Table II where we give, for 30 levels originating from the $4f^86p$ configuration, both the theoretical values obtained without (HFR) and with (HFR+CP) core-polarization effects. It is seen that the polarization does generally increase the lifetime values by about 30%. The agreement is very good (in fact within the experimental errors) when comparing the measurements of the present work with the HF+CP results and appears as a quite remarkable result if one keeps in mind the difficulty of calculating the lifetime values for such complicated atomic structures.

Considering the experimental lifetime values and the theoretical branching fractions as obtained in the present work, it is possible to derive normalized transition probabilities. In Table IV, we present the transition probabilities for the strongest lines ($\log_{10} gf>-1.0$) depopulating the levels for which the experimental lifetimes are reported in Table II. We include, in the table, the air wavelength (in Å), as deduced from the tabulated energy levels [24], the upper and lower levels of the transitions with the parity and J value, the weighted oscillator strengths on the logarithmic scale ($\log_{10} gf$), and the weighted transition probabilities (gA), both normalized with the laser measurements of the present work. It has been verified that all the transitions quoted in Table IV are not affected by cancellation effects in the calculation of the line strengths and, consequently, the corresponding transition probabilities are expected to be accurate within a few percent. Table IV includes some transitions of astrophysical interest and a table containing a larger number of transitions is available in the database DREAM [30].

Due to their importance for magnetic field investigations in some stars, we give, in Table V, the calculated Landé factors for some low-lying levels ($E<20\,000\ \text{cm}^{-1}$) of Tb III. There are no other data available for comparison.

IV. CONCLUSIONS

A set of transition probabilities has been obtained for the $5d$-$6p$ and $6s$-$6p$ transitions depopulating four levels of Tb III belonging to the $4f^8(^7F)6p$ configuration. These A values have been determined from a combination of experimental lifetimes and HFR branching fractions but the theoretical model has been assessed by a comparison with experimental lifetimes measured by laser-induced fluorescence spectroscopy at the Lund Laser Center (Lund, Sweden). The agreement observed between theory and experiment strongly supports the set of theoretical lifetimes for the 30 levels considered and the corresponding A values obtained in the present work and stored in the DREAM database. The accuracy of the transition probabilities, depending mostly upon the uncertainties of the theoretical branching fractions, is expected to be within a few percent for the strongest lines. The uncertainties of the results for the weaker transitions could be larger for some transitions but their final assessment would require accurate experimental branching fractions for all the transitions concerned. These data are expected to help the physicists involved in the study of the crystalline structure of RE salts and to provide the astrophysicists with some atomic data needed for improving the determination of the chemical composition of chemically peculiar stars.

ACKNOWLEDGMENTS

This work was financially supported by the Swedish Natural Science Research Council and by the EU-TMR Access to Large-Scale Facilities program (Contract No. HPRI-CT-1999-00041). Financial support from the Belgian FNRS is acknowledged by E.B., P.Q., and H.-P.G.

[1] A. Dupont, J. Opt. Soc. Am. **57**, 867 (1967).
[2] C. R. Cowley, T. Ryabchikova, F. Kupka, D. J. Bord, G. Mathys, and W. P. Bidelman, Mon. Not. R. Astron. Soc. **317**, 299 (2000).
[3] P. Swings, Astrophys. J. **100**, 132 (1944).
[4] G. C. L. Aikman, C. R. Cowley, and H. M. Crosswhite, Astrophys. J. **232**, 812 (1979).
[5] S. J. Adelman and S. N. Shore, Publ. Astron. Soc. Pac. **93**, 85 (1981).
[6] C. R. Cowley and M. Greenberg, Mon. Not. R. Astron. Soc. **232**, 763 (1988).
[7] R. D. Cowan, *The Theory of Atomic Structures and Spectra* (University of California Press, Berkeley, CA, 1981).
[8] E. Biémont, Z. S. Li, P. Palmeri, and P. Quinet, J. Phys. B **32**, 3409 (1999).
[9] Z. S. Li, H. Lundberg, G. M. Wahlgren, and C. M. Sikström, Phys. Rev. A **62**, 032505 (2000).
[10] Z. G. Zhang, A. Persson, Z. S. Li, S. Svanberg, and Z. K. Jiang, Eur. Phys. J. D **13**, 301 (2001).
[11] E. Biémont, H. P. Garnir, T. Bastin, P. Palmeri, P. Quinet, Z. S. Li, Z. G. Zhang, V. Lokhnygin, and S. Svanberg, Mon. Not. R. Astron. Soc. **321**, 481 (2001).
[12] E. Biémont, H. P. Garnir, P. Palmeri, P. Quinet, Z. S. Li, Z. G. Zhang, and S. Svanberg, Phys. Rev. A **64**, 022503 (2001).
[13] P. Palmeri, P. Quinet, Y. Frémat, J.-F. Wyart, and E. Biémont, Astrophys. J., Suppl. **129**, 367 (2000).
[14] Z. S. Li, Z. G. Zhang, V. Lokhnygin, S. Svanberg, T. Bastin, E. Biémont, H. P. Garnir, P. Palmeri, and P. Quinet, J. Phys. B **34**, 1349 (2001).
[15] E. Biémont, H. P. Garnir, Z. S. Li, V. Lokhnygin, P. Palmeri, P. Quinet, S. Svanberg, J.-F. Wyart, and Z. G. Zhang, J. Phys. B **34**, 1869 (2001).
[16] Z. G. Zhang, Z. S. Li, S. Svanberg, P. Palmeri, P. Quinet, and E. Biémont, Eur. Phys. J. D **15**, 301 (2001).
[17] Z. G. Zhang, Z. S. Li, H. Lundberg, K. Y. Zhang, Z. W. Dai, Z. K. Jiang, and S. Svanberg, J. Phys. B **33**, 521 (2000).
[18] Z. G. Zhang, S. Svanberg, P. Palmeri, P. Quinet, and E. Biémont, Astron. Astrophys. (to be published).
[19] Z. G. Zhang, G. Somesfalean, S. Svanberg, P. Palmeri, P. Quinet, and E. Biémont, Astron. Astrophys. (to be published).
[20] E. Biémont, P. Palmeri, P. Quinet, G. Paquin, Z. G. Zhang, G. Somesfalean, and S. Svanberg, Mon. Not. R. Astron. Soc. **328**, 1085 (2001).
[21] A. W. Weiss, Phys. Rev. A **51**, 1067 (1995).
[22] R. E. Irving, M. Henderson, L. J. Curtis, I. Martinson, and P. Bengtsson, Can. J. Phys. **77**, 137 (1999).
[23] E. Meinders, T. A. M. van Kleef, and J.-F. Wyart, Physica (Amsterdam) **61**, 443 (1972).
[24] W. C. Martin, R. Zalubas, and L. Hagan, *Atomic Energy Levels—The Rare Earth Elements*, Natl. Bur. Stand. Ref. Data Ser., Natl. Bur. Stand. Stand. (U.S.) Circ. No. 60 (U.S. GPO, Washington, DC, 1978).
[25] J.-F. Wyart, in *Laboratory and Astronomical High Resolution Spectra*, ASP Conf. Ser., Vol. 81, edited by A. J. Sauval and N. Grevesse (Astronomical Society of the Pacific, San Francisco, 1995).
[26] L. Brewer, J. Opt. Soc. Am. **59**, 2083 (1971).
[27] J.-F. Wyart and C. Bauche-Arnoult, Phys. Scr. **22**, 583 (1981).
[28] S. Fraga, J. Karwowski, and K. M. S. Saxena, *Handbook of Atomic Data* (Elsevier, Amsterdam, 1976).
[29] P. Quinet, P. Palmeri, E. Biémont, M. M. McCurdy, G. Rieger, E. H. Pinnington, M. E. Wickliffe, and J. E. Lawler, Mon. Not. R. Astron. Soc. **307**, 934 (1999).
[30] http://www.umb.ac.be/~astro/dream.shtml